Calmodulin Binding to Myosin Light Chain Kinase Begins at Substoichiometric Ca^{2+} Concentrations: A Small-Angle Scattering Study of Binding and Conformational Transitions†

Joanna K. Krueger,‡ Nicholas A. Bishop,‡ Donald K. Blumenthal,§ Gang Zhi,|| Kathy Beckingham,⊥ James T. Stull,|| and Jill Trewhella*,‡

Chemical Science and Technology Division, Mail Stop G758, Los Alamos National Laboratory, Los Alamos, New Mexico 87545, and Department of Biochemistry and Cell Biology, Rice University, Houston, Texas 77251, and Physiology Department, University of Texas Southwestern Medical Center, Dallas, Texas 75235, and Department of Pharmacology and Toxicology, University of Utah, Salt Lake City, Utah 84112

Received July 13, 1998; Revised Manuscript Received October 15, 1998

ABSTRACT: We have used small-angle scattering to study the calcium dependence of the interactions between calmodulin (CaM) and skeletal muscle myosin light chain kinase (MLCK), as well as the conformations of the complexes that form. Scattering data were measured from equimolar mixtures of a functional MLCK and CaM or a mutated CaM (B12QCaM) incompetent to bind Ca^{2+} in its N-terminal domain, with increasing Ca^{2+} concentrations. To evaluate differences between CaM−enzyme versus CaM−peptide interactions, similar Ca^{2+} titration experiments were performed using synthetic peptides based on the CaM-binding sequence from MLCK (MLCK-I). Our data show there are different determinants for CaM binding the isolated peptide sequence compared to CaM binding to the same sequences within the enzyme. For example, binding of either CaM or B12QCaM to the MLCK-I peptide is observed even in the presence of EGTA, whereas binding of CaM to the enzyme requires Ca^{2+}. The peptide studies also show that the conformational collapse of CaM requires both the N and C domains of CaM to be competent for Ca^{2+} binding as well as interactions with each end of MLCK-I, and it occurs at ∼2 mol of Ca^{2+}/mol of CaM. We show that CaM binding to the MLCK enzyme begins at substoichiometric concentrations of Ca^{2+} (≤2 mol of Ca^{2+}/mol of CaM), but that the final compact structure of CaM with the enzyme requires saturating Ca^{2+}. In addition, MLCK enzyme does bind to $2Ca^{2+}$·B12QCaM, although this complex is more extended than the complex with native CaM. Our results support the hypothesis that CaM regulation of MLCK involves an initial binding step at less than saturating Ca^{2+} concentrations and a subsequent activation step at higher Ca^{2+} concentrations.

Calmodulin (CaM)[1] is responsible for the Ca^{2+}-dependent regulation of a wide range of cellular processes via its interactions with a diverse array of target enzymes. CaM binds four calcium ions which induces conformational changes that increase its affinity for target proteins and lead to complex formation and activation or inactivation of numerous biochemical pathways (*1, 2*). CaM has a dumbbell-shaped structure in which two globular lobes, termed the N and C domains, are linked by a single seven-turn, solvent-exposed α-helix (*3, 4*) that is flexible in solution (*5, 6*). Each globular lobe contains two helix-loop-helix structures that serve to bind Ca^{2+}, with the C-terminal lobe having ∼6-fold higher Ca^{2+} affinity (*7*). Upon binding Ca^{2+}, a hydrophobic cleft is exposed in each globular lobe that interacts with hydrophobic residues in the target protein (*6, 8*−*12*). The two primary interactions between $4Ca^{2+}$·CaM and peptides based on CaM-binding sequences from many of its targets involve residues in the N-terminus of the peptide interacting with the C domain of CaM and residues in the C-terminus of the peptide interacting with the N domain of CaM. The binding of different target peptides or proteins "tunes" the Ca^{2+}-binding affinities of the two CaM domains, enhancing the difference in binding affinities between them (*13, 14*). The activation by CaM of several of its target

† This work was performed under the auspices of the Department of Energy under contract to the University of California and was supported by DOE project KP1101010 (J.T.) and NIH grants GM40528 (J.T.), HL26043 (J.T.S.), GM49155 (K.B.) and a grant from the Robert A. Welch Foundation of Texas (K.B.). X-ray scattering data were obtained at the Stanford Synchrotron Research Laboratory using instrumentation supported by the DOE (Basic Energy Sciences and Office of Health and Environmental Research) and the NIH Biomedical Resource Technology Program, Division of Research Resources.

* To whom correspondence should be addressed.
‡ Los Alamos National Laboratory.
§ University of Utah.
|| University of Texas Southwestern Medical Center.
⊥ Rice University.

[1] Abbreviations: B12QCaM, mutant calmodulin inactivated for Ca^{2+} binding in the N-terminal domain by site specific mutations Glu67Gln and Glu31Gln; CaM, calmodulin; DTT, dithiothreitol; d_{max}, maximum linear dimension; EGTA, ethylene glycol bis(β-aminoethyl ether)-*N*,*N*,*N*′,*N*′-tetraacetic acid; I_0, forward or zero angle scattering; MLCK, myosin light chain kinase; MOPS, 3-(*N*-morpholino)propanesulfonic acid; tBOC, *tert*-butyloxycarbonyl; TFA, trifluoracetic acid; R_g, radius of gyration.

10.1021/bi981656w CCC: $15.00
Published on Web 12/01/1998

enzymes has been examined using kinetic analyses (*16*−*19*). In each case, it was concluded that occupancy of three or four sites is necessary for activation. These studies did not differentiate between activation and binding, however. Several other early spectroscopic and fluorescence investigations have shown that CaM can interact with its target proteins at submaximal Ca^{2+} concentrations and have proposed novel conformations of CaM (*20*, *21*) as well as target protein binding (*22*) at intermediate Ca^{2+} concentrations.

One of the most studied examples of CaM enzyme regulation is that of myosin light chain kinase (MLCK) activation. MLCK contains a catalytic core followed immediately by a carboxyl-terminal regulatory segment consisting of both an autoinhibitory sequence and a CaM-binding sequence (*23*−*25*). In its inactive conformation, the regulatory segment of MLCK maintains numerous contacts with the catalytic core, thus inhibiting substrate binding (*26*−*28*). Small-angle X-ray and neutron scattering (*29*), NMR (*30*), and X-ray crystallography (*9*) of CaM complexed with peptides based on CaM-binding sequences from smooth and skeletal muscle MLCKs demonstrate that CaM undergoes a conformational collapse that is achieved via the flexibility in the interconnecting helix region that allows the two lobes of CaM to come into close contact and encompass the peptide. Recent neutron-scattering experiments (*31*) have shown that $4Ca^{2+}$·CaM undergoes an identical, unhindered conformational collapse upon binding a catalytically competent form of MLCK and that CaM activates MLCK by inducing a significant movement of the kinase's regulatory segment away from the surface of the catalytic core. This CaM-induced movement then allows the kinase to bind and close about its substrate (*32*). Bayley et al. (*13*) demonstrated the kinetic plausibility of a $2Ca^{2+}$·CaM·MLCK intermediate using short peptide sequences based on the two halves of the CaM-binding sequence from skeletal muscle MLCK. Similar conclusions were drawn by Peersen et al. (*14*) from their kinetic studies of CaM interactions with intact MLCK and five different peptides. The question posed is whether binding of CaM to MLCK and activation of MLCK by CaM are sequential steps in the regulatory mechanism. Since the C domain of CaM has the higher Ca^{2+} affinity, the focus has been on interactions between the Ca^{2+}-loaded C domain and its target binding sequence for the initial binding step.

We have completed a set of small-angle X-ray scattering experiments aimed at further understanding MLCK activation by Ca^{2+}/CaM and obtaining evidence for whether this regulation involves a $2Ca^{2+}$·CaM·MLCK intermediate as has been proposed. The scattering of a particle in solution at zero angle, or the forward scattering (I_0), is very sensitive to changes in the size of the scattering particle due to, for example, complex formation, specific oligomerization, or aggregation. We used the forward scattering to evaluate, as a function of Ca^{2+} concentration, the binding of CaM to (1) a catalytically functional N-terminal truncation mutant of skeletal muscle MLCK (*33*); (2) MLCK-I, the 25-residue peptide corresponding to the CaM-binding domain of skeletal muscle MLCK (*34*); and (3) a truncated version of the skeletal muscle CaM-binding domain designated (N-5)-MLCK-V. To assess the different roles of Ca^{2+}-binding to the C domain versus N domain of CaM in CaM−MLCK interactions, a mutated CaM, B12QCaM (*35*), incompetent for binding Ca^{2+} in its N domain was also studied. The scattering intensity as a function of angle [$I(Q)$ vs Q] was used to determine the overall shapes of any complexes that formed between CaM and the MLCK enzyme or the peptides. These data provide insights into the role that Ca^{2+} plays in CaM binding to MLCK as well as in inducing conformational transitions necessary to activate its targets.

MATERIALS AND METHODS

Protein and Peptide Preparation. MLCK (residues 257−607 of the skeletal muscle form; 40 kDa) was purified as described by Gao et al. (*33*) with the addition of an FPLC gel filtration (S12, Pharmacia) step. Column elution buffer was treated with Chelex-100 to remove Ca^{2+} ions and contained 20 mM MOPS, pH 7.5, 25 mM KCl, 2.5 mM magnesium chloride (added after Chelex treatment), 1 mM DTT, and 2.5% glycerol. Only plastic containers, rinsed with the divalent cation chelator, EGTA, were utilized for all buffer and protein samples. Several stock buffer solutions containing varying amounts of Ca^{2+} were prepared by addition of $CaCl_2$ to the Chelex-treated column elution buffer. Exact concentrations of Ca^{2+} and Mg^{2+} in each stock buffer solution were determined by atomic absorption emission. In all cases the concentration of Mg^{2+} was 2.5 mM as expected.

Ca^{2+}-free calmodulin was prepared as described by Heidorn et al. (*29*). Ca^{2+}-free B12QCaM was prepared as described by Maune et al. (*36*), with the addition of a final HPLC C-18 purification step. Both CaM and B12QCaM were allowed to come to equilibrium in a buffer containing 0.5 M EGTA and then dialyzed extensively against the above Chelex-treated buffer. All protein concentrations were confirmed by comparing small-angle scattering I_0 measurements to those of a standard protein of known concentration, monodisperse, and measured in the same sample cell on the same day (see below).

Lyophilized MLCK-I peptide (KRRWKKNFIAVSAANRFKKISSGAL; 2964.5 Da) was brought up in and dialyzed (in 300 MW cutoff dialysis tubing) against the Chelex-treated FPLC column elution buffer. Final concentrations were determined from absorption measurements at 280 nm. (N-5)-MLCK-V (KAFIAVSAAARFG-amide; 1308.6 Da) was designed by omitting 5 N-terminal residues from the MLCK-V peptide sequence [KRRWKKAFIAVSAAARFG (*37*)]. Thus, (N-5)MLCK-V is missing the conserved tryptophan essential for binding to the C domain of CaM. MLCK-V was originally designed based on the minimal skeletal muscle MLCK CaM-binding sequence [KRRWKKNFIAVSAAARF (*37*, *38*)]. (N-5)MLCK-V was synthesized using tBOC chemistry, purified by reversed-phase HPLC using a Vydac C4 column with a gradient of 0.1% TFA water/0.1% acetonitrile. The composition of the purified peptide was confirmed by amino acid analysis. Lyophilized (N-5)MLCK-V peptide was brought up in the Chelex-treated FPLC buffer, however, since it is missing the N-terminal tryptophan, absorption at 215 and 258 nm was monitored during purification off the HPLC column prior to lyophilization. These values were used to estimate the amount of (N-5)MLCK-V peptide available. Due to the possibility of losing peptide during dialysis and the difficulty of measuring (N-5)MLCK-V concentrations, these samples were not dialyzed.

Samples for Scattering Experiments. Scattering data were collected using 10−15 μL samples loaded into a quartz

capillary and containing equimolar CaM and MLCK enzyme (27 μM each), CaM/MLCK-I peptide (220 μM each), CaM/(N-5)MLCK-V peptide (360 μM each), B12QCaM/MLCK enzyme (26 μM each), B12QCaM/MLCK-I (160 μM each), or B12QCaM (240 μM each). Because the scattering signal is proportional to the square of the molecular weight of the scattering particle, lower concentrations could be used for the CaM/enzyme measurements to avoid enzyme aggregation. The quartz capillaries were rinsed with EGTA prior to loading samples. Although careful attention was paid to eliminating Ca^{2+} from all buffers and proteins, background Ca^{2+} levels were estimated as ~1 mol of Ca^{2+}/mol of CaM in the samples. This estimate was based on a comparison of the changes in R_g values and $P(r)$ profiles determined from scattering data collected at Los Alamos with those determined from comparable experiments done at the SSRL (Stanford Synchrotron Radiation Line) while using an EGTA-buffered system (see below). Background Ca^{2+} levels were most likely due to the fact that we were using small volumes and dilute samples. In addition, we chose not to use an EGTA buffer in the final experiments in order to avoid potential complications in interpreting the results arising from possible interactions between EGTA and the proteins (*39*−*42*). As a result of the background Ca^{2+} contamination, only the samples containing 5 mM EGTA without added Ca^{2+} have apo-CaM. Further, since the protein concentrations used in this study are much greater than the K_D values for Ca^{2+} binding to CaM, most of the Ca^{2+} present will be bound to CaM in the absence of EGTA.

Small-Angle X-ray Scattering Data Acquisition and Analysis. X-ray scattering data were collected using the X-ray instrument at Los Alamos described in Heidorn and Trewhella (*5*), as well as beam line 4-2 at the SSRL (*43*). Comparison of the synchrotron data with data measured on the same sample preparations at Los Alamos using the much weaker sealed-tube X-ray source showed signs of radiation damage due to the high X-ray intensities at the synchrotron source. Specifically, there was evidence for mild radiation-induced aggregation in the CaM/MLCK enzyme samples. A concentration series was necessary for each of the Ca^{2+}-free CaM and B12QCaM preparations as interparticle interference effects were observed in the scattering data for those buffer conditions. Interparticle interference occurs when the surface charge of the scattering particle is such that nearby particles are repulsed. This effect results in suppression of the scattering intensity at the smallest angles (*44*) and generally can be eliminated by measuring scattering data over a range of concentrations and extrapolating to infinite dilution.

X-ray scattering data were reduced to $I(Q)$ versus Q and analyzed as described in Heidorn and Trewhella (*5*). $I(Q)$ is the scattered X-ray intensity per unit solid angle, and Q is the amplitude of the scattering vector. Q is equal to $(4\pi \sin \theta)/\lambda$, where 2θ is the scattering angle and λ is the wavelength of the scattered X-rays (1.542 Å for the CuKα used). The inverse Fourier transform of $I(Q)$ yields $P(r)$, which is the frequency of vector lengths connecting small-volume elements within the entire volume of the scattering particle.

$$P(r) = (1/2\pi^2) \int I(Q) Qr \sin (Qr)\, dQ \qquad (1)$$

$P(r)$ goes to zero at the maximum linear dimension of the particle, d_{max}. $P(r)$ profiles were calculated using the method of Moore (*45*). The radius of gyration, R_g, and forward scatter, I_0, were calculated from the second and zero moments of $P(r)$, respectively. R_g is defined as the root-mean-square of all elemental volumes from the center-of-mass of the particle, weighted by their scattering densities. I_0 is directly proportional to the molar particle concentration multiplied by the square of its molecular weight for particles with the same mean scattering density.

Evaluation of Samples for Aggregation and Complex Formation. Extraction of structural information on individual proteins or protein complexes in solution from scattering data requires samples that are rigorously free of nonspecific aggregates. I_0 values derived from X-ray scattering data of all samples reported herein were compared with those of a standard protein [lysozyme (*46*) or CaM (*5*)] measured in the same sample cell on the same day to ensure samples were aggregation free. I_0 values used to determine concentrations were calculated after extrapolation of the data to infinite dilution for each of the samples that showed evidence for interparticle interference.

The I_0 values determined for each of the standard proteins were also used to calculate an expected I_0 value for each of the potential complexes: CaM/MLCK, CaM/MLCK-I, and CaM/(N-5)MLCK-V. For comparison, the expected I_0 value for samples of uncomplexed components can be calculated as a percent of the expected I_0 value for samples in which the components are fully complexed using the known molecular weights of each component (M_1 and M_2) and the following relationship:

$$I_0 \text{ (uncomplexed)} = [M_1^2 + M_2^2/(M_1 + M_2)^2] I_0 \text{(complexed)} \qquad (2)$$

Note that the molar concentrations are not part of this equation because in our experiments equimolar concentrations of each component were used. Thus, the I_0 values expected for uncomplexed mixtures of CaM/MLCK, CaM/MLCK-I, and CaM/(N-5)MLCK-V are 58, 74.4, and 86.5% of the expected I_0 value for each complex, respectively. Likewise, the I_0 value for a solution of dimers will be four times that for a solution of monomers, provided the specific volumes of the two forms are equivalent. For a monomer−dimer mixture (*47*), the forward scatter [$I_{0(m-d)}$] can be expressed in terms of I_0 for the monomer [$I_{0(m)}$] and the mole fraction of dimers in the sample, f:

$$I_{0(m-d)} = I_{0(m)}[(3f + 1)/(f + 1)] \qquad (3)$$

where f is given by

$$f = c_d/(c_d + c_m) \qquad (4)$$

and c_m and c_d are the monomer and dimer molar concentrations, respectively.

RESULTS

CaM/Peptide Studies. Scattering data were measured for mixtures of CaM or B12QCaM with MLCK-I peptide in 5 mM EGTA and as a function of Ca^{2+} added without EGTA. Table 1 summarizes the R_g, d_{max}, and I_0 values determined for each sample, while Figures 1 and 2 show the respective

Table 1: Ca^{2+} Dependence of Scattering Parameters for CaM or B12QCaM Mixed with MLCK-I Peptide

	mol of Ca^{2+}/mol of CaM[a]	R_g (Å)[b]	measured I_0/I_0 (complex)[b,c]	d_{max} (Å)	comment
CaM/MLCK-I	0 + 5 mM EGTA[d]	19.2 ± 0.2	1.03 ± 0.01	65	complexed, extended conformation
	1	19.2 ± 0.4	0.90 ± 0.04	63	complexed, extended conformation
	2	18.2 ± 0.2	0.88 ± 0.04	56	complexed, extended conformation
	3	17.7 ± 0.2	0.89 ± 0.04	56	complexed, extended conformation
	4	18.4 ± 0.2	1.01 ± 0.04	57	complexed, extended conformation
	5	18.0 ± 0.2	0.94 ± 0.04	56	complexed, extended conformation
	7	17.9 ± 0.2	0.94 ± 0.04	57	complexed, extended conformation
	11	18.2 ± 0.2	0.97 ± 0.04	57	complexed, extended conformation
B12QCaM/MLCK-I	0 + 5mM EGTA[d]	22.1 ± 0.20	0.97 ± 0.01	70	complexed, extended conformation
	1	20.2 ± 0.9	0.91 ± 0.07	67	complexed, extended conformation
	6	25.4 ± 0.9	1.36 ± 0.06	85	extended conformation evidence for 2(B12QCaM)/MLCK-I

[a] These values, as well as those in Table 2, are estimates of total Ca^{2+} concentrations taking into account that background Ca^{2+} concentrations can be up to 1 mol of Ca^{2+}/mol of CaM. See Materials and Methods. [b] Errors in R_g and I_0 are based on counting statistics only. Additional contributions to the error in I_0 are possible due to uncertainties in protein or peptide concentration. [c] The expected I_0 for uncomplexed CaM/MLCK-I = $0.74I_0$ of the complex. [d] Data on 0 added Ca^{2+} plus 5 mM EGTA were collected at SSRL, all other data were collected at Los Alamos.

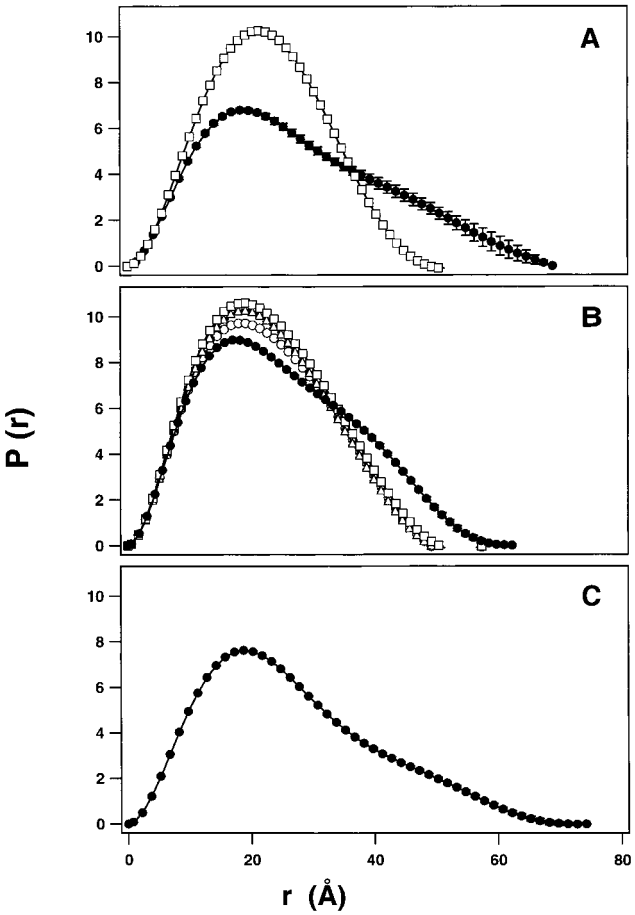

FIGURE 1: $P(r)$ functions from X-ray scattering data obtained using the instrument at Los Alamos for (A) CaM with 1 mol Ca^{2+}/mol CaM (●); (B) CaM/MLCK-I with 1 (●), 2 (○), 3 (△), and 5 (□) mol of Ca^{2+}/mol of CaM; and (C) CaM/(N-5)MLCK-V with 6.5 (●) mol of Ca^{2+}/mol of CaM. The data for CaM with 1 mol of Ca^{2+} bound were collected at several concentrations and extrapolated to infinite dilution to remove interparticle interference effects. For comparison, panel A also shows the $P(r)$ calculated for the NMR solution structure of CaM·MLCK-I (□).

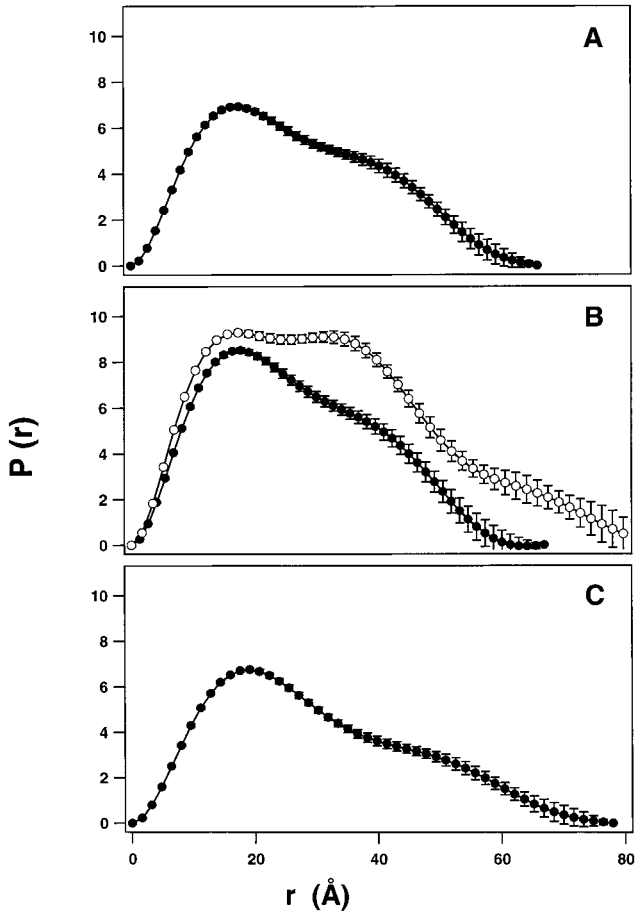

FIGURE 2: $P(r)$ functions from X-ray scattering data obtained using the instrument at Los Alamos for (A) B12QCaM with 1 mol of Ca^{2+}/mol of CaM (●); (B) B12QCaM/MLCK-I with 1 (●) and 6 (○) mol Ca^{2+}/mol of CaM; and (C) B12QCaM/(N-5)MLCK-V with 4.5 (●) mol of Ca^{2+}/mol of CaM. The data for B12QCaM with 1 mol of Ca^{2+} bound was collected at several concentrations and extrapolated to infinite dilution to remove interparticle interference effects.

$P(r)$ functions. In addition to these mixtures, scattering data were obtained for B12QCaM and CaM alone since the solution structure for the mutant B12QCaM had not previously been characterized. The respective $P(r)$ profiles for CaM (Figure 1A) and B12QCaM (Figure 2A) each have a bimodal shape with a peak at ~18 Å, a shoulder at ~40 Å, and a d_{max} of ~67 Å, all of which are characteristic of the dumbbell-shaped CaM in solution (*5*). The scattering data are therefore consistent with B12QCaM and CaM having similar overall conformations. The R_g value for B12QCaM in the absence of Ca^{2+} is 20.5 ± 0.6 Å, which is the same within error as the value of 21.2 ± 0.6 Å measured for CaM under identical solution conditions. These R_g values are

slightly larger than the values previously published for CaM, most likely due to different solvent conditions. The buffer used in this study had a lower ionic strength and included glycerol. Glycerol accentuates the hydration layer effects around the protein complexes giving rise to larger apparent R_g and d_{max} values (*48*).

The I_0 values for the CaM/MLCK-I mixture (220 μM each) (Table 1) show that $\geq$90% of the CaM is bound to the peptide even in the presence of EGTA. Furthermore, $P(r)$ analyses (Figure 1B) show that CaM completely collapses about MLCK-I with only ~2 mol of Ca^{2+}/mol of CaM. The R_g and d_{max} values for the compact CaM/MLCK-I structure are slightly larger than the values reported for deuterated CaM complexed with MLCK-I (*29*) again because of the different solvent conditions. Scattering data on mixtures of B12QCaM and MLCK-I peptide (160 μM each) in EGTA, as well as with $\leq$1 mol of Ca^{2+}/mol of CaM, also gave I_0 values consistent with those expected for a $\geq$90% complexed B12QCaM/MLCK-I (Table 1). At saturating Ca^{2+} levels, I_0 measured for the B12QCaM/MLCK-I mixture is ~1.4 times that expected for a 1:1 B12QCaM/MLCK-I complex. Further, the corresponding $P(r)$ (Figure 2B) shows a dramatic increase in the frequency of vector lengths around 35 Å and a large increase in d_{max}. The larger than expected I_0 value as well as the extended $P(r)$ profile indicate aggregates or associations of >1 CaM/peptide. One possibility is that, under the conditions of the scattering experiments, the Ca^{2+}-bound C-terminal lobe of B12QCaM is capable of binding to both ends of the MLCK-I peptide. Assuming this is what happens and using eqs 3 and 4, we calculate that the mole fraction of B12QCaM/MLCK-I/B12QCaM complexes in the sample is 0.31 $\pm$ 0.01.

Scattering data measured for mixtures of CaM or B12QCaM (360 and 240 μM, respectively) with (N-5)MLCK-V peptide in EGTA and with increasing Ca^{2+} concentrations in the absence of EGTA were inconclusive concerning the Ca^{2+} dependence of the peptide binding. The (N-5)MLCK-V peptide is small (1.9 kDa) and the expected change in the measured I_0 for uncomplexed versus complexed CaM, or B12QCaM, with (N-5)MLCK-V is only 13%. This value is close to the combined systematic and statistical errors in these particular experiments. The principal source of systematic error in the I_0 analysis is in the determination of the concentrations for the peptide and CaM components, and the (N-5)MLCK-V peptide is the most problematic for determining accurate concentrations (see Materials and Methods). Consistent with binding of the peptide, under saturating Ca^{2+} conditions, we did see small increases in the long vector length region of the $P(r)$ functions for both CaM and B12QCaM mixed with (N-5)MLCK-V (Figures 1C and 2C, respectively) compared to those of the proteins in the absence of the peptide (Figures 1A and 2A, respectively). Importantly, the $P(r)$ functions show that neither CaM nor B12QCaM collapses about the (N-5)MLCK-V peptide at saturating Ca^{2+} concentrations.

The Ca^{2+} titration experiments described here for the CaM/peptide mixtures were each repeated using independent sample preparations at SSRL, with and without an EGTA buffer. The conclusions and results of which (not shown) are similar to those given here.

CaM/MLCK Enzyme Studies. Scattering data were measured for mixtures of CaM and MLCK enzyme (27 μM each) in 5 mM EGTA as well as with increasing Ca^{2+} concentrations in the absence of EGTA. A representative sampling of the corresponding $P(r)$ functions are shown in Figure 3, while Table 2 summarizes the I_0, R_g, and d_{max} values for all samples measured. Comparison of the $P(r)$ profiles for MLCK (Figure 3A) and for CaM/MLCK at 0 mol of Ca^{2+} *added* with and without 5 mM EGTA (Figure 3B) confirms our estimate of ~1 mol of Ca^{2+}/mol of CaM present in the background. A similar change in the $P(r)$ profile was observed in the EGTA-buffered experiments at SSRL between 0 and 1 mol of bound Ca^{2+} compared with the EGTA and 0 Ca^{2+} added experiments shown here.

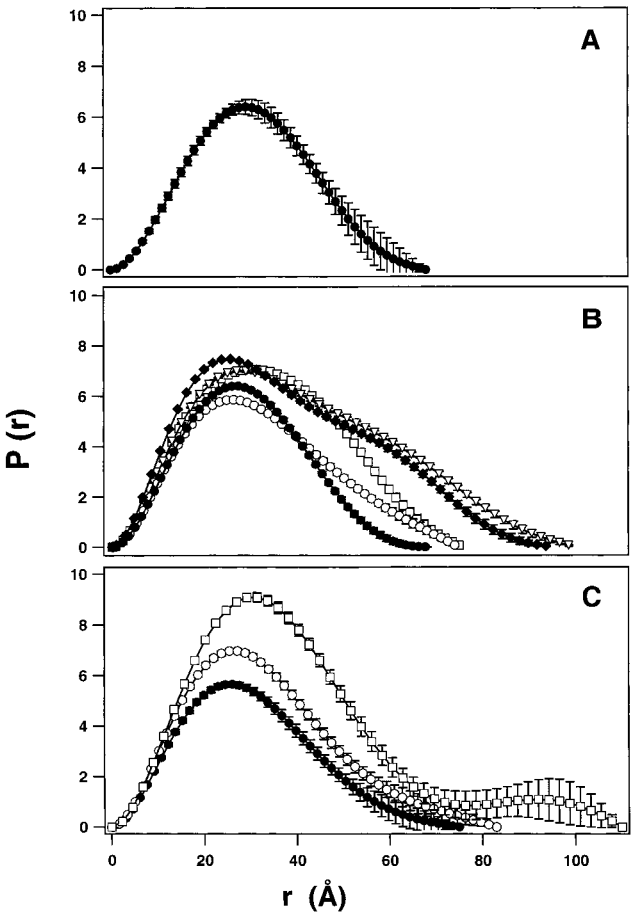

FIGURE 3: $P(r)$ functions from X-ray scattering data obtained using the instrument at Los Alamos for (A) MLCK by itself; (B) CaM/MLCK with 5 mM EGTA (●), 1 (○), 1.7 (□), 2.5 (▽), and 6 (◆) mol of Ca^{2+}/mol CaM; and (C) B12QCaM/MLCK with 5 mM EGTA (●), with 1 (○), and 5 (□) mol of Ca^{2+}/mol of CaM. The 2.5 mol Ca^{2+}/mol of CaM data is an average of three data sets with between 2.3 and 2.8 mol of Ca^{2+}/mol of CaM.

The ratios of the measured I_0 values for CaM/MLCK mixtures at each Ca^{2+} concentration to that expected for a fully complexed CaM/MLCK (Table 2) show that CaM is capable of binding to MLCK when ~1.7 mol of Ca^{2+} is present, although there is on average less than 1 mol of CaM bound/mol of MLCK at these levels. For the ~1 mol of Ca^{2+}/mol of CaM sample, the $P(r)$ profile and the R_g value indicate some evidence for binding, but it is below the limit that can be quantitated from the I_0 analysis. Evidence for full binding, i.e., 1 mol of CaM bound/mol of MLCK, occurs with ~2.5 mol of Ca^{2+} present. $P(r)$ analysis of these data indicates that the average shape of the complexes present is similar to that seen for the complex with saturating Ca^{2+} (i.e. = 4

Table 2: Ca^{2+} Dependence of CaM or B12QCaM Mixed with MLCK Enzyme

	mol of Ca^{2+}/mol of CaM	R_g (Å)	measured I_0/I_0 (complex)[a]	d_{max} (Å)	comment
CaM /MLCK	0 + 5mM EGTA	22.4 ± 0.80	0.55 ± 0.05	70	uncomplexed
	1	25.0 ± 0.95	0.59 ± 0.06	75	minimal, if any, complex formation
	1.7	26.2 ± 0.71	0.79 ± 0.06	76	some complex formation
	2.5[b]	32.6 ± 0.90	0.97 ± 0.06	100	complexed
	4	29.5 ± 1.70	0.98 ± 0.08	100	complexed
	6	29.4 ± 1.70	0.93 ± 0.07	95	complexed
B12QCaM/MLCK	0 + 5mM EGTA	23.5 ± 1.2	0.52 ± 0.06	75	uncomplexed
	1[c]	26.5 ± 3.2	0.69 ± 0.06	89	some complex formation; extended conformation
	5	31.4 ± 2.50	1.02 ± 0.09	110	complexed extended conformation

[a] The expected I_0 for uncomplexed CaM/MLCK = $0.58I_0$ for the complex. [b] Average of three data sets each with between 2−3 mol of Ca^{2+}/mol of CaM. [c] Average of two data sets each with 1 mol of Ca^{2+}/mol of CaM.

mol of Ca^{2+} present). There is, however, a distinctive shift in peak position from about 30 Å to around 26 Å, a shortening of d_{max} by about 5 Å, and a decrease in the R_g value from 32.6 ± 0.9 to 29.4 ± 1.7 Å for the Ca^{2+}-saturated complex (Figure 3B, Table 3). These observed changes are indicative of a CaM/MLCK complex that has adopted its final, maximally compact structure necessary for substrate binding and phosphorylation.

Scattering data were measured for equimolar mixtures of B12QCaM and MLCK enzyme (26 μM each) with 0 and saturating Ca^{2+} added, as well as in EGTA. The I_0 values (Table 2) measured for the mixtures of B12QCaM and MLCK enzyme show that B12QCaM does not bind MLCK in the presence of EGTA, but does begin to bind in the presence of only 1 mol of Ca^{2+}/mol of CaM as evidenced by increases in the I_0 and R_g values. $P(r)$ analysis (Figure 3C and Table 2) of the Ca^{2+}-saturated $2Ca^{2+}$·B12QCaM·MLCK complex shows that although full complex formation has been achieved, the resultant structure is quite extended with an R_g value of 31.4 Å and a d_{max} reaching to 110 Å.

Experiments done at SSRL in an EGTA-buffered system gave qualitatively similar results for the Ca^{2+} titrations on CaM/MLCK and CaM/B12QCaM complexes, but with evidence for some radiation-induced aggregation of the enzyme due to the high intensity of the synchrotron source.

DISCUSSION

Early kinetic studies have shown that CaM can interact with its target proteins at submaximal Ca^{2+} concentrations without effecting enzyme activation (*18*, *20*, *22*). More recently, Bayley and co-workers (*13*) have proposed a general mechanism for CaM−target enzyme interactions based on their kinetic observations involving Ca^{2+} and CaM interactions with short peptide sequences from the two halves of the target sequence of skeletal muscle MLCK. They suggest the existence of an intermediate inactive CaM−enzyme complex at resting Ca^{2+} concentrations whereby CaM maintains an interaction with the enzyme, via its C domain, for the full range of physiological Ca^{2+} concentrations. Changes in cytoplasmic Ca^{2+} concentrations could then be used to control the N domain interaction required for regulation. In this way, activation of the intermediate complex by transient increases in Ca^{2+} could be prompt and efficient since CaM would be constrained from diffusing away from its binding site on the enzyme. Peersen et al. (*14*) also proposed a mechanism involving a $2Ca^{2+}$·CaM·MLCK intermediate based on kinetic analyses using the full-length skeletal MLCK as the CaM target. Similar conclusions were drawn by Johnson et al. (*49*) from their studies of the kinetics of Ca^{2+} binding to a number of CaM target proteins and peptides. Our studies describe the structural changes of several CaM−MLCK complexes at various Ca^{2+} concentrations, a summary of which is illustrated in Figure 4. The results affirm that CaM binds to MLCK at substoichiometric Ca^{2+} concentrations (~2 mol of Ca^{2+}/mol of CaM) but does not attain its final compact conformation unless saturating Ca^{2+} concentrations are present. This evidence supports the hypothesis that one molecule of CaM may tether itself, via its C domain, to an inactive molecule of MLCK at subsaturating concentrations of Ca^{2+} in cells. Such an intermediate structure would be positioned for immediate response to a rise in Ca^{2+} with occupancy of Ca^{2+}-binding sites in the N domain of CaM.

The proposed tethering or anchoring function by one lobe of CaM is reminiscent of the mechanism proposed for the Ca^{2+}-dependent regulation of troponin I by troponin C based on neutron scattering contrast variation studies (*50*). Troponin C is evolutionarily related and structurally homologous to CaM and functions as part of the troponin complex in regulating the interactions between the thick and thin filaments of muscle. The C domain of troponin C has two orders of magnitude higher affinity for Ca^{2+} than the N-terminal regulatory domain. The C domain is therefore always occupied at physiological Ca^{2+} concentrations in muscle. The neutron-derived solution structure of the troponin C/troponin I complex, in the presence of saturating Ca^{2+}, shows troponin C to have an extended conformation with troponin I forming a super-helical structure that winds its way through the hydrophobic clefts in each lobe of troponin C. We proposed that the N domain of troponin C regulates the interaction of troponin I with the thin filament actin molecules by alternately binding and releasing troponin I, while the C-terminal lobe anchors or tethers the troponin complex to the thin filament assembly.

It should be noted that for samples containing CaM with less than saturating Ca^{2+} concentrations we could be measuring the average scattering from a mixture of structures with varying amounts of bound Ca^{2+}. The precise distribution of species would depend on the equilibrium constants for Ca^{2+}-binding to CaM in the presence of MLCK enzyme or peptide. Without target peptides or proteins present, the C-terminal domain of CaM binds Ca^{2+} with only 6-fold higher affinity than the N-terminal domain (*7*). However, several studies (*13*, *14*, *49*) have shown that the presence of different target peptides can tune the Ca^{2+}-binding affinities and kinetics of the two CaM domains such that the N-terminal domain will

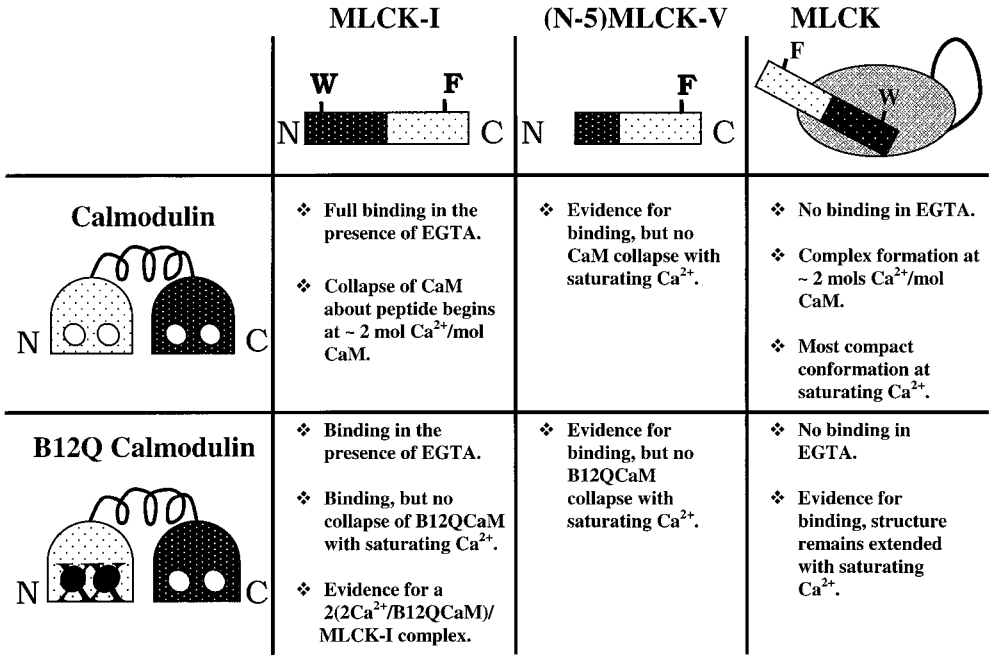

FIGURE 4: Summary of Ca^{2+}-dependence of peptide and enzyme binding to CaM.

bind Ca^{2+} significantly more weakly than the C-terminal domain. Since the C-terminal domain of CaM loads with Ca^{2+} first, we expect the $2Ca^{2+}$·CaM·MLCK structure to be a significant proportion of the species present. To ensure a pure $2Ca^{2+}$·CaM species, we performed additional experiments utilizing B12QCaM that is incompetent for binding Ca^{2+} in its N domain. In these experiments, we do see clear evidence for a $2Ca^{2+}$·CaM·MLCK complex. However, the overall shape function [$P(r)$] for the complex shows differences with respect to the corresponding complex with native CaM in the vector length region >50 Å. The differences indicate that B12QCaM does not form a compact globular complex with MLCK. The extended "tail" region in the $P(r)$ suggests that one of the CaM lobes may not associate with the MLCK but rather is flexibly tethered to the enzyme.

In sharp contrast to what we observed for the MLCK enzyme, the isolated MLCK-I peptide is capable of binding to CaM, as well as B12QCaM, even in the presence of EGTA. Kataoka and colleagues (*51*) previously observed binding of the venom peptide mellitin, which models many of the features of CaM-binding domains in target enzymes, to CaM in EGTA using small-angle X-ray scattering. Ever since CaM-binding proteins and peptides were first purified using CaM affinity columns, it has been clear that there is an inherent difference in the binding of CaM-binding peptides versus intact proteins (*34*). Many investigators have noted that these peptides bind tightly to CaM affinity columns and that extensive washing of the column with high concentrations of EGTA is insufficient to remove the peptide from the column. Rather, denaturants as well as high concentrations of EGTA are required.

Both the MLCK-I peptide and MLCK formed complexes with Ca^{2+}/B12QCaM, although the resultant complexes remain extended and their scattering profiles are different from the analogous CaM complexes at intermediate Ca^{2+} concentrations. In particular, there is evidence suggesting a 2($2Ca^{2+}$·B12QCaM)/MLCK-I complex may form, i.e., a 2:1 complex between B12QCaM and MLCK-I. One possible mechanism by which such a complex could form would be for the competent C domain of B12QCaM to bind to both ends of the MLCK-I peptide giving rise to a peptide-bridged double CaM complex. On the basis of calculations from the scattering data, up to 30% of the CaM molecules, and hence 15% of the peptide, could participate in the proposed peptide bridged structure at 160 μM protein and peptide concentration values. The question arises as to why would two CaM molecules would preferentially bind to one peptide in the presence of excess free peptide? Barth et al. (*52*) in their fluorescence study utilizing isolated N and C domains of CaM showed that two molecules of either domain can bind to CaM-binding peptides based on MLCK-I with either peptide polarity. They further showed that binding of the C domain of CaM to the peptide via interactions with the conserved Trp residue at the N-terminus of the peptide induces full helicity in the peptide. This conformational change may account for why a second B12QCaM molecule might bind preferentially to the C-terminal end MLCK-I rather than to excess free peptide that would be unstructured and conformationally flexible. The proposed interaction between the C domain of B12QCaM and the C terminal end of MLCK-I must be of lower affinity and hence not significantly competitive with the "normal" interaction between the peptide's N-terminus and the C domain of native CaM. Binding of B12QCaM at each end of the CaM-binding sequence was not observed with the MLCK enzyme probably because of limited accessibility in the intact enzyme restricting simultaneous access to both ends of the CaM-binding sequence.

Our scattering data show that the binding of CaM requires either the N-terminus or the C-terminus of the MLCK-I peptide for CaM recognition and binding. In contrast, induction of the collapse of CaM about its target binding sequence requires interactions between each of the N and C domains of CaM with the C- and N-terminal MLCK-I

sequence, respectively. Further, the peptide studies show that CaM completely collapses about the peptide at ~2 mol of Ca^{2+}/mol of CaM. We also conclude that there are CaM-binding properties specific for the intact enzyme that the shorter isolated peptide sequences do not possess. It would appear that more Ca^{2+} is required for CaM binding to disrupt interactions between the regulatory sequence of MLCK and the surface of the catalytic core than is required for CaM to simply bind to its isolated peptide sequence. Zhi et al. (*53*) recently showed that the type of catalytic core, not the CaM binding sequence per se, determined the sensitivity to CaM activation of CaM-dependent protein kinase II and MLCKs. Thus, there appear to be additional interactions between CaM and the catalytic core of these kinases that are important for activation. Alternatively, one could also argue that interactions between the MLCK regulatory sequences and the catalytic domain "compete" with CaM interactions at low Ca^{2+}, allowing CaM to easily dissociate in the absence of Ca^{2+}, and bind (but not activate) at intermediate Ca^{2+} concentrations.

ACKNOWLEDGMENT

We wish to thank Sue Rokop for preparation of CaM and B12QCaM. We thank Dr. H. Tsurata for assistance in X-ray scattering data acquisition at SSRL. Beneficial discussions with Peter Bayley are also gratefully acknowledged.

REFERENCES

1. Crivici, A., and Ikura, M. (1995) *Annu. Rev. Biophys. Biomol. Struct. 24*, 85−116.
2. James, P., Vorherr T., and Carafoli E. (1995) *Trends Biochem. Sci. 20*, 38−42.
3. Babu, Y. S., Sack, J. S., Greenhough, T. J., Bugg, C. E., Means, A. R., and Cook, W. J. (1985) *Nature 315*, 37−40.
4. Babu, Y. S., Bugg, C. E., and Cook, W. J. (1988) *J. Miol. Biol. 204*, 191−204.
5. Heidorn, D. B., and Trewhella, J. (1988) *Biochemistry 27*, 909−915.
6. Barbato, G., Ikura, M., Kay, L. E., Pastor, R. W., and Bax, A. (1992) *Biochemistry 31*, 5269−5278.
7. Linse, S., Helmersson, A., and Forsen, S. (1991) *J. Biol. Chem. 266*, 8050−8054.
8. Strynadka, N. C. J., and James, M. N. G. (1988) *Proteins: Struct., Funct., Genet. 3*, 1−17.
9. Meador, W. E., Means, A. R., and Quiocho, F. A. (1992) *Science 257*, 1251−1255.
10. Finn, B. E., Evenäs, J., Drakenberg, T., Waltho, J. P., Thulin, E., and Forsén, S (1995) *Nat. Struct. Biol. 2*, 777−783.
11. Kuboniwa, H., Tjandra, N., Grzesiek, S., Ren, H., Klee, C. B., and Bax, A. (1995) *Nat. Struct. Biol. 2*, 768−776.
12. Zhang, M., Tanaka, T., and Ikura, M. (1995) *Nat. Struct. Biol. 2*, 758−767.
13. Bayley, P., Findlay, W. A., and Martin, S. R. (1996) *Protein Sci. 5*, 1215−1228.
14. Peersen, O. B., Madsen, T. S., and Falke, J. J. (1997) *Protein Sci. 6*, 794−807.
15. Huang, C. H., Chau, V., Chock, P. B., Wang, J. H., and Sharma, R. K. (1981) *Proc. Natl. Acad. Sci. U.S.A. 78*, 871−874.
16. Cox, J. A., Malnoe, A., and Stein, E. A. (1981) *J. Biol. Chem. 256*, 3218−3222.
17. Cox, J. A., Comte, M., and Stein, E. A. (1982) *Proc. Natl. Acad. Sci. U.S.A.* 79, 4265−4269.
18. Burger, D., Stein, E. A., and Cox, J. A. (1983) *J. Biol. Chem. 258*, 4733−4739.
19. Blumenthal, D. K., and Stull, J. T. (1982) *Biochemistry 21*, 2386−2391.
20. Mackall, J., and Klee, C. B. (1991) *Biochemistry 30*, 7242−7247.
21. Burger, D., Cox, J. A., Comte, M., and Stein, E. A. (1984) *Biochemistry 23*, 1966−1971.
22. Kincaid, R. L., and Vaughn, M. (1986) *Proc. Natl. Acad. Sci. U.S.A. 83*, 1193−1197.
23. Edelman, A. M., Takio, K., Blumenthal, D. K., Hansen, R. S., Walsh, K. A., Titani, K., and Krebs, E. G. (1985) *J. Biol. Chem. 260*, 1275−1285.
24. Kemp, B. E., Parker, M. W., Hu, S., Tiganis, T., and House, C. (1994) *Trends Biochem. Sci. 19*, 440−444.
25. Stull, J. T., Krueger, J. K., Zhi, G., and Gao, Z.-H. (1995) in *International Symposium on Regulation of the Contractile Cycle in Smooth Muscle*, MIE, Japan.
26. Krueger, J. K., Padre, R. C., and Stull, J. T. (1995) *J. Biol. Chem. 270*, 16848−16853.
27. Gallagher, P. J., Herring, B. P., Trafny, A., Sowadski, J., and Stull, J. T. (1993) *J. Biol. Chem. 268*, 26578−26582.
28. Kemp, B. E., and Pearson, R. B. (1991) *Biochim. Biophys. Acta 1094*, 67−76.
29. Heidorn, D. B., Seeger, P. A., Rokop, S. E., Blumenthal, D. K., Means, A. R., Crespi, H., and Trewhella, J. (1989) *Biochemistry 28*, 6757−6764.
30. Ikura, M., Clore, G. M., Gronenborn, A. M., Zhu, G., Klee, C. B., and Bax, A. (1992) *Science 256*, 632−638.
31. Krueger, J. K., Olah, G. A., Rokop, S. E., Zhi, G., Stull, J. T., and Trewhella, J. (1997) *Biochemistry 36*, 6017−6023.
32. Krueger, J. K., Zhi, G., Stull, J. T., and Trewhella, J. (1998*) Biochemistry 37*, 13997−14004.
33. Gao, Z.-H., Zhi, G., Herring, B. P., Moomaw, C., Deogny, L., Slaughter, C. A., and Stull, J. T. (1995) *J. Biol. Chem. 270*, 10125−10135.
34. Blumenthal, D. K., Takio, K., Edelman, A. M., Charbonneau, H., Titani, K., Walsh, K. A., and Krebs, E. G. (1985) *Proc. Natl. Acad. Sci. 82*, 3187−3191.
35. Mukherjea, P., Maune, J. F., and Beckingham, K. (1996) *Protein Sci. 5*, 468−477.
36. Maune, J. F., Klee, C. B., and Beckingham, K. (1992) *J. Biol. Chem. 267*, 5286−5295.
37. Dasgupta M., Honeycutt T., and Blumenthal D. K. (1989) *J. Biol. Chem. 264*, 17156−17163.
38. Blumenthal, D. K., and Krebs, E. G. (1987) *Methods Enzymol. 139*, 115−126.
39. Haiech, J., Derancourt, J., Pechere, J.-F., and Demaille, J. G. (1979) *Biochemistry 18*, 2752−2758.
40. Kronman, M. J., and Bratcher, S. C. (1983) *J. Biol. Chem. 258*, 5707−5709.
41. Kronman, M. J. (1989) *Crit. Rev. Biochem. Mol. Biol. 24*, 565−667.
42. Stemmer, P., and Klee, C. B. (1990) *FEBS Lett. 276*, 71−74.
43. Wakatsuki, S., Hodgson, K. O., Eliezer, D., and Rice, M. (1992) *Rev. Sci. Instrum. 63*, 1736−1740.
44. Wu, C.-F., and Chen, S.-H. (1988) *Biopolymers 27*, 1065−1083.
45. Moore, P. B. (1980) *J. Appl. Crystallogr. 13*, 168−175.
46. Kringbaum, W. R., and Kugler, F. R. (1970) *Biochemistry 9*, 1216−1223.
47. Hubbard, S. R., Hodgson, K. O., and Doniach, S. (1988) *J. Biol. Chem. 263*, 4151−4158.
48. Lehmann, M. S., and Zaccai, G. (1984) *Biochemistry 23*, 1939−1942.
49. Johnson, D. J., Synder, C., Walsh, M., and Flynn M. (1996) *J. Biol. Chem. 271*, 761−767.
50. Olah, G. A., and Trewhella, J. (1994) *Biochemistry 33*, 12800−12806.
51. Kataoka, M., Head, J. F., Seaton, B. A., and Engelman, D. M. (1989) *Proc. Natl. Acad. Sci U.S.A. 86*, 6944−6948.
52. Barth, A., Martin, S. R., and Bayley, P. M. (1998) *J. Biol. Chem. 273*, 2174−2183.
53. Zhi, G., Abdullah, S. M., and Stull, J. T. (1998) *J. Biol. Chem. 273*, 8951−8957.

BI981656W